Journal of Cardiovascular Medicine and Cardiology

LJ Vallez[1], B Sun[1], BD Plourde[1], JP Abraham[1]* and CS Staniloae[2]

[1]University of St. Thomas School of Engineering, 2115 Summit Ave, St. Paul, MN 55105-1079, USA
[2]NYU Langone Medical Center, 333 East 38th St. New York, NY 10016, USA

**Dates:** **Received:** 03 December, 2015; **Accepted:** 08 December, 2015; **Published:** 12 December, 2015

***Corresponding author:** J.P. Abraham, University of St. Thomas School of Engineering, 2115 Summit Ave, St. Paul, MN 55105-1079, E-mail: JPABRAHAM@stthomas.edu

**www.peertechz.com**

**Keywords:** Artery compliance; Cardiovascular disease; Atherectomy; Heart disease; Blood flow; Hemodynamics

**ISSN:** 2455-2976

Research Article

# Numerical Analysis of Arterial Plaque Thickness and its Impact on Artery Wall Compliance

**Abstract**

A numerical analysis was completed on the influence of plaque on the compliance of an artery wall. The analysis allowed a systematic variation of the transluminal pressure difference and plaque thickness. Included in the analysis was a sheath of surrounding tissue that provides support during the cyclical deformation. The analysis incorporated progressively thicker layers of plaque to quantify their impact on the artery compliance. It was found that the presence of plaque plays a significant role in reducing the compliance. It is also shown that modest reductions in plaque thickness can result in large changes in the compliance and a positive health outcome. The calculations also included only a health artery (absence of plaque). The healthy artery possessed the largest compliance of the cases. The healthy-artery results were compared with literature and found to be in good agreement. The calculations were made with four different transmural pressure variations to capture the entire range of possible values. The results for all pressure waveforms agreed qualitatively although there was some difference in magnitude.

## Introduction

Cardiovascular disease is a major cause of mortality throughout the world. The history of cardiovascular research is rich and although this study is not intended to be a review of the subject, a short summary related to the present work is necessary. Interested readers are invited to review articles such as [1-4]. These studies are representative of the literature which deal with the complexities of hemodynamics. Among the important subtopics are the relationship between the wall and the fluid. The fluid exerts a shear stress on the wall which is believed to be a causing of thickening of the wall and the initiation of cardiovascaular disease. The flow also has an impact on transport through the arterial wall [5-20].

In addition to these hemodynamic-focused studies, it has been found that arterial compliance (the distension of an artery wall during the cardiac cycle) is an important indicator of disease progression. In particular, for a diseased artery, the stiffened arterial wall or the rigid plaque layer reduces the otherwise healthy-artery response to pressure fluctuations [21-22]. In addition, the presence of a stenosis can affect the blood velocity profile [21-26] which can be measured Doppler or ultrasound techniques [27-37].

The above-mentioned fluid-wall interaction is two-way in that the fluid affects the wall and the wall in turn affects the flow. This interaction is often termed “two way fluid structural interaction (two way FSI)”. Incorporating the two-way interaction is currently an active area of research [38-59].

Among these references, the majority treat the artery as an isolated structure with stress-free conditions on the exterior surface and upstream and downstream surfaces that are able to move radially but not axially. Insofar as the surrounding tissue does exert an influence on the artery as it is subjected to cardiac-cycle pressure, it may be important to include the tissue in the analysis. To the best knowledge of the authors, three studies have investigated this issue. In [57], the pressure of the surrounding tissue was incorporated into the analysis by means of an exterior non-zero pressure. In [58], the surrounding tissue was modeled with a viscoelastic support along the artery. Most recently [59], a systematic study was completed to vary the thickness of the surrounding artery wall until further changes to its thickness no longer impacted the results. It was found that the presence of plaque significantly reduces the compliance of the artery and that for a healthy artery, a 6.5 mm sheath is required. Omission of the surrounding tissue resulted in a significant over prediction of the compliance.

The present study is aimed at determining how removal of plaque changes the artery compliance. There has been a recent advance in atherectomy procedures and techniques [15,60-66]. The procedures have been shown to remove plaque, open clogged arteries, and increase flow rate. What is less known is the impact of plaque removal on the artery-wall compliance. If the effect of these treatments on compliance can be quantified, it can greatly add in the determination of treatment for patients.

### Mathematical model

In the present analysis, the finite element technique will be combined with experimental data obtained from patients (pre- and post-treatment arterial and plaque dimensions). The targeted artery is the popliteal. The experiments provided pre- and post-operative flow and pressure information upstream and downstream of a superficial femoral artery lesion. In addition, the diameter and cross sectional areas upstream, downstream, and within the lesion were found.

Standard lower extremity angiography of the entire vascular tree was performed. The Combo Wire® (Volcano Corporation) was

normalized at the level of common femoral artery, and then placed in the distal popliteal artery, just proximal to the take-off of the anterior tibial artery.

The resting gradient was recorded. A blood pressure cuff was positioned at the calf level and inflated for 1 minute at 10 mmHg above the systolic blood pressure. After cuff deflation, the hyperemic gradient was recorded. At that time, an IVUS catheter (Volcano Corporation) was passed across the lesion. The reference vessel diameter was measured in the normal arterial segment just proximal to the lesion. The minimal luminal area was measured at the narrowest point inside the lesion. Once the procedure was completed, the pressure wire was repositioned in the same segment of the popliteal artery, and measurements were repeated. Case files were collected and archived on the ComboMap® console from Volcano Corporation.

The simulated geometry is shown in Figure 1. The figure shows a three-part solution domain that includes calcified plaque, artery wall tissue, and surrounding tissue. The thicknesses of the artery wall and the surrounding tissue and the material properties are from [59]. They are listed here in Table 1. Linear elastic properties have been shown to suitably calculate artery deformation [50]. In [59], it was shown that the results are not sensitive to the value of the Poisson ratio. There, it was also shown that the required thickness of the surrounding sheet was 6.5 mm and that value is used through this study. The mechanical properties are listed in Table 1.

The plaque was assumed to be uniformly presented around the lumen so that axisymmetry could be used. To reduce solution time and increase spatial resolution, an angle of 10 degrees was used. This assumption of axisymmetry is not a limitation of the modeling; if the tangential deployment of the plaque deposit is known, it can be incorporated into the analysis.

## Boundary conditions

At the upstream and downstream ends of the artery and tissue, radial motion was allowed but axial motion was prohibited. The external conditions are less obvious; it is not clear what the value of the external pressure should be since in some cases, the artery is internal to the organisms and therefore the far-field pressure is non-zero. In other cases, the vessels are near the skin surface so not only would there be a non-axisymmetric pressure but over part of the exterior the pressure would be zero. It is recognized that the superficial femoral artery is deep within tissue and an external pressure approximately equal to the diastolic pressure would be most suitable. In an effort to provide results which are of more general value, we will define the external pressure systematically with values that vary from zero to the diastolic pressure. The pressure within the lumen is taken from measurements. To simplify the mathematics, the software will require the translumen pressure and not the separate pressures at the two surfaces. Here we define four cases which are listed in Table 2. In the Table, $P_{ineternal}$ refers to the pressure inside the artery.

## The numerical model

**Time discretization:** The solutions were initialized to a zero stress state and five cardiac cycles (Figures 2,3) were input. The time stepping was performed with different values to ensure time-step independence. Time step values of .01, .05, and .1 seconds were used and deformation of the artery wall was found to differ by less than 1 % throughout the cycle. For the remaining solutions to be reported, time steps of .1 seconds were employed.

**Spatial discretization:** The finite element solution requires a spatial discretization of the solution domain. A sequence of meshes were used that were increasingly refined. The refinements incorporated a 20-fold increase in the numbers of elements. The solutions from these various levels of refinement differed by less than 2 % so that a mesh independence was obtained. The results to be presented correspond to approximately 1700 number of elements for a 10 degree wedge (approximately 62,000 for a fully circular domain). The exact number of elements varied slightly among the simulations because the size of the lesion varied. Figure 3 has been prepared to show a view of the mesh with annotations calling out the regions.

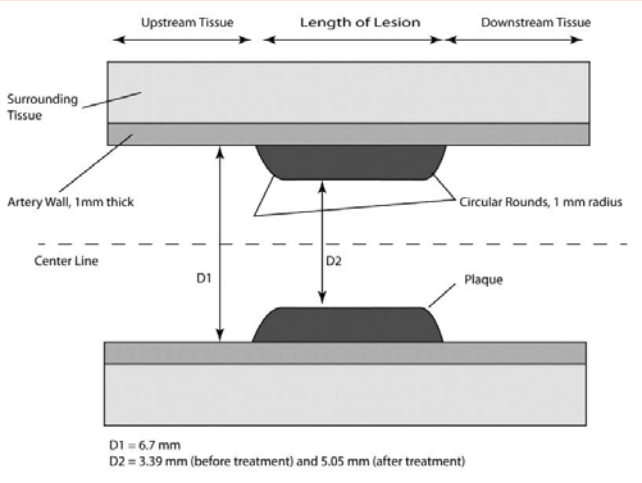


**Figure 1:** Schematic of the solution domain.



*Citation:* *Vallez LJ, Sun B, Plourde BD, Abraham JP, Staniloae CS (2015) Numerical Analysis of Arterial Plaque Thickness and its Impact on Artery Wall Compliance. J Cardiovasc Med Cardiol 2(2): 026-034. DOI: 10.17352/2455-2976.000019*

**Table 1:** Material properties.

| Material | Young's Modulus (MPa) | Poisson Ratio | Density |
|---|---|---|---|
| Plaque | 12.6 | 0.3 | 1000 |
| Artery Wall | 1 | 0.3 | 1000 |
| Surrounding Tissue | 1 | 0.3 | 1000 |

**Table 2:** Definition of the translumen pressure differences used in the simulations.

| Case | External Pressure (torr) | Internal | Translumen pressure |
|---|---|---|---|
| 1 | 0 | From measurement | Pinternal – 0 torr |
| 2 | 20 | From measurement | Pinternal – 20 torr |
| 3 | 40 | From measurement | Pinternal – 40 torr |
| 4 | diastolic | From measurement | Pinternal – Pdiasolic |

**Solution domain size:** One issue which needs to be addressed is the size of the solution domain which is required to ensure that boundary conditions there do not influence the results. With respect to the radial extent, it was previously shown that a 6.5 mm thick surrounding tissue zone was sufficient to ensure accuracy [59]. The axial extent (annotated in Figure 1) was determined by systematically enlarging the domain and repeating compliance calculations until further enlargements did not influence results. All the results to be provided in the following section correspond to a sufficiently large axial extent. It should be noted however that in reality, arteries are not straight. There is a tortuosity that varies from patient to patient. In addition, the axisymmetric lesion is also idealized; in reality, the lesion may vary in thickness along its length and is often deployed non-symmetric within the artery. The results obtained here are consequently idealized.

## Results and Discussion

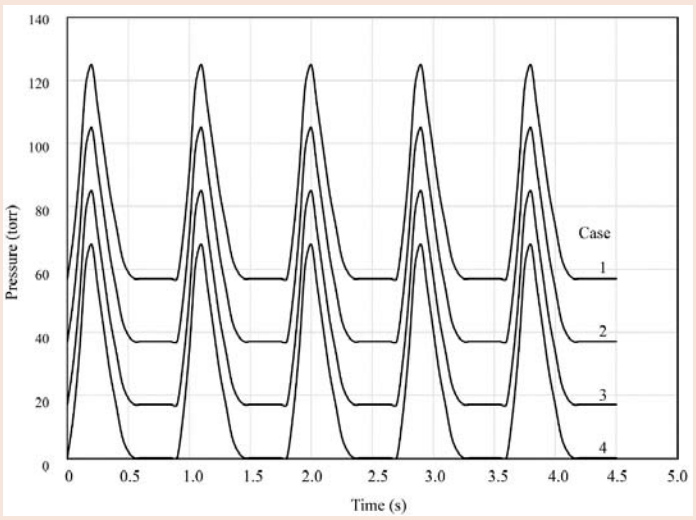


**Figure 2:** Translumen pressure difference for the cases of Table 2 prior to plaque removal treatment.

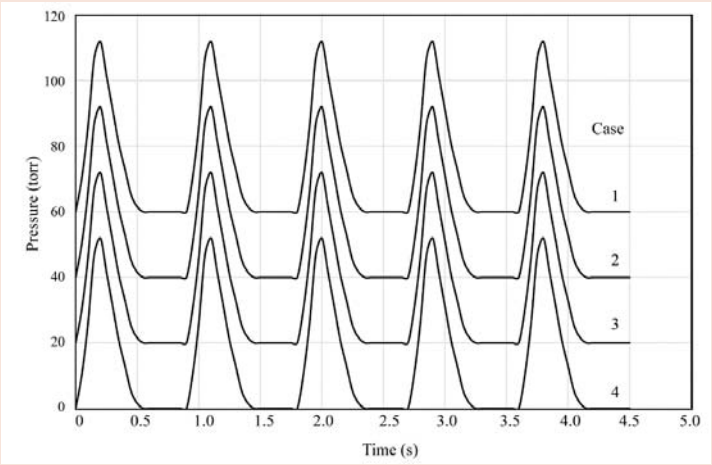


**Figure 3:** Translumen pressure difference for the cases of Table 2 after plaque removal treatment.



*Citation:* *Vallez LJ, Sun B, Plourde BD, Abraham JP, Staniloae CS (2015) Numerical Analysis of Arterial Plaque Thickness and its Impact on Artery Wall Compliance. J Cardiovasc Med Cardiol 2(2): 026-034. DOI: 10.17352/2455-2976.000019*

The primary result to be presented is the compliance of the artery wall for the various pressure and plaque thickness situations. The compliance is calculated by the radial deformation of the inner plaque surface. The definition of area compliance, from [66], is

$$Area\,Compliance = \frac{\Delta Area}{\Delta Pressure} \quad (1)$$

Where $\Delta Area$ is the increase of area during the cardiac cycle and ΔPressure is the transmural pressure difference. Another commonly used measure of compliance is the diametrical compliance which is defined as

$$Diametrical\,Compliance = 10,000 \bullet \frac{\Delta D / D}{\Delta Pressure} \quad (2)$$

The Diamond Back 360° Peripheral Orbital Atherectomy System (OAS; Cardiovascular Systems, Inc) was used to modify the surface of calcified plaque while preserving the more elastic arterial wall. The differential sanding property results in plaque fracture, luminal enlargement, and very low balloon inflation pressure, minimizing injury to the vessel wall. Lesion pretreatment with the OAS has translated into a decreased need for bail-out stenting, which preserves the opportunity for future revascularization treatments. For more detailed information on the peripheral orbital atherectomy device and clinical data [66].

In this case, we used a 2.0mm crown which was initially activated at 60,000 rotation / min. After 2 passes, the orbital speed was increased to 90,000 rotations/min. The plaque removal procedure was terminated after the final 2 passes at 120,000 rotations/min. The activation time was 30 seconds per pass (180 seconds for the entire treatment), with a pause of 30 seconds in between passes. The atherectomy result was checked via angiogram, and the residual stenosis was measured with the IVUS.

To aid in the discussion, tables have been created to categorize the many individual calculations. The first table (Table 3) presents results for translumen pressure variation Case 1. There it is seen that the presence of plaque has a significant impact on the deformation (plaque reduces compliance). It is also seen that the length of the lesion is not important except for very short lengths (3 mm). The results for 7, 12, and 18 mm lesions are indistinguishable.

With respect to improvements achieved by plaque removal, it is seen that for the pre-operative plaque thickness, the area compliance is approximately 0.1% however the post-operative case (plaque thickness of 0.825 mm, the compliance has tripled (increased by 200%). Only a modest reductions in plaque thickness with orbital atherectomy resulted in large changes in the compliance.

If attention is turned to the subsequent tables, the same conclusions can be drawn. Reductions in plaque thickness markedly alter the compliance. Furthermore, with the exception of very short lesions, the length of the lesion does not influence the results. It is also seen that the magnitude of the transmural pressure difference is positively related to the deformation with larger values of transmural pressure giving rise to larger deformation. This result is expected.

The compliance is weakly dependent on the transmural pressure at these pressure levels because of the appearance of the pressure difference in the denominator. There is a slight increase in compliance for the smallest transmural pressure differences, this finding is confirmed by literature [67].

Insofar as the popliteal artery is deep within perfused tissue, the most appropriate external pressure value is diastolic (corresponds to Case 4). The other cases correspond to arteries which would be close to the skin surface.

In these tables, the symbols ΔA, ΔP, and ΔD refer to changes of artery cross section area, change in pressure, and change in diameter during a cardiac cycle.

A graphical display of a subset of the results is provided in Figure 5. There, the results correspond to pressure Case 4 which typifies a deep-tissue artery such as the superficial femoral. There, two curves are shown that reveal the decrease of compliance with increase in calcified plaque thickness. The curves are annotated for plaque lesions 7 mm and longer and for a plaque lesion of 3 mm. It is seen that there is a very slight dependence of the results on plaque lesion length but a much more substantive dependence on plaque thickness.

## Comparison of present calculations with measurements

It is important to compare these results with expectations from the literature. While there it is difficult to find a perfect comparison because of the differences from patient to patient and the paucity of high-quality quantifiable results, it was possible to find a reasonable comparison candidate [67]. A comparison of these results with

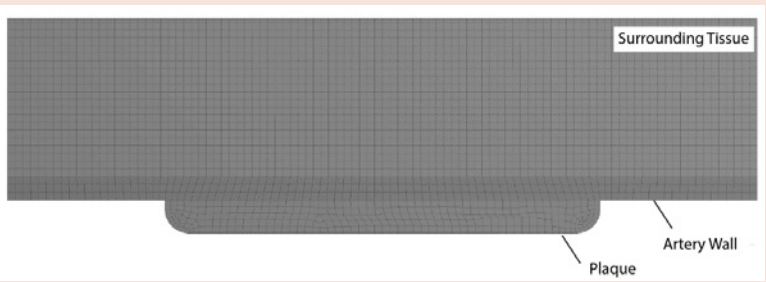


**Figure 4:** Solution domain and discretization mesh.

**Table 3:** Results for transluminal pressure Case 1.

| Case | Plaque Thickness (mm) | Plaque Length (mm) | Inner Diameter (mm) | Area Compliance (ΔA/ΔP) ($mm^2$/torr) % | Diameter Compliance ΔD/D/ΔP) X$10^4$ |
|---|---|---|---|---|---|
| 1 | 1.66 | 3 | 3.38 | 0.10 | 2.22 |
| 2 | 1.66 | 7 | 3.38 | 0.08 | 1.69 |
| 3 | 1.66 | 12 | 3.38 | 0.08 | 1.68 |
| 4 | 1.66 | 18 | 3.38 | 0.08 | 1.74 |
| 5 | 1.39 | 3 | 3.92 | 0.15 | 2.47 |
| 6 | 1.39 | 7 | 3.92 | 0.12 | 1.90 |
| 7 | 1.39 | 12 | 3.92 | 0.11 | 1.87 |
| 8 | 1.39 | 18 | 3.92 | 0.12 | 1.90 |
| 9 | 0.825 | 3 | 5.05 | 0.33 | 3.25 |
| 10 | 0.825 | 7 | 5.05 | 0.27 | 2.72 |
| 11 | 0.825 | 12 | 5.05 | 0.27 | 2.65 |
| 12 | 0.825 | 18 | 5.05 | 0.27 | 2.68 |
| 13 | 0.413 | 3 | 5.87 | 0.63 | 4.61 |
| 14 | 0.413 | 7 | 5.87 | 0.56 | 4.12 |
| 15 | 0.413 | 12 | 5.87 | 0.55 | 4.04 |
| 16 | 0.413 | 18 | 5.87 | 0.55 | 4.06 |
| 17 | 0 | 3 | 6.70 | 1.17 | 6.56 |
| 18 | 0 | 7 | 6.70 | 1.17 | 6.56 |
| 19 | 0 | 12 | 6.70 | 1.17 | 6.56 |
| 20 | 0 | 18 | 6.70 | 1.17 | 6.56 |

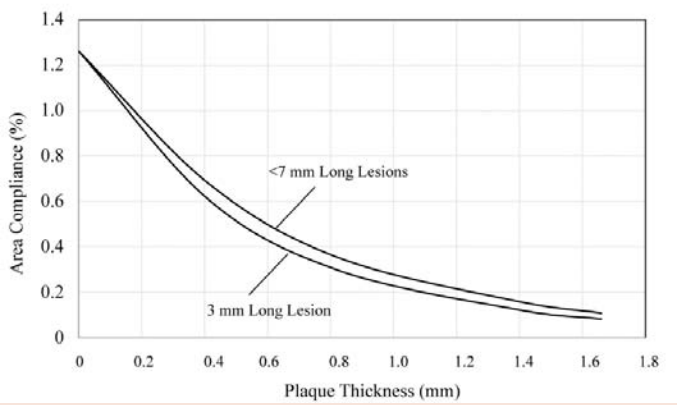


**Figure 5:** Dependence of area compliance on plaque thickness for pressure variation Case 4.

[67], shows very good agreement, lending support to the present calculations.

A further comparison is made with [68]. They find a health population proximal superficial femoral artery compliance of 3.1 – 9.1% which compares well to the results of Table 6 without plaque. While it is difficult to compare the diseased population of [69], with the diseased results of this study because little information was given about the thickness, type, and length of plaque regions in [67], nevertheless, the lower range of their diametrical compliance values (3.1%) agree well with moderate diseased case (Cases 9-16 of Table 6) that were provided here.

## Study limitations

While the results presented in this paper give clear guidance connecting the thickness of calcified plaque and arterial compliance, the plaque model was simplified as both axisymmetric and with a flat profile. While the internal dimensions matched those from patient measurements, in truth the non-uniform distribution is expected to lead to results that may differ from this generalized simplified case.


*Citation:* *Vallez LJ, Sun B, Plourde BD, Abraham JP, Staniloae CS (2015) Numerical Analysis of Arterial Plaque Thickness and its Impact on Artery Wall Compliance. J Cardiovasc Med Cardiol 2(2): 026-034. DOI: 10.17352/2455-2976.000019*

**Table 4:** Results for transluminal pressure Case 2.

| Case | Plaque Thickness (mm) | Plaque Length (mm) | Inner Diameter (mm) | Area Compliance (ΔA/ΔP) ($mm^2$/torr) % | Diameter Compliance (ΔD/D/ΔP) $X10^4$ |
|---|---|---|---|---|---|
| 1 | 1.66 | 3 | 3.38 | 0.10 | 1.86 |
| 2 | 1.66 | 7 | 3.38 | 0.08 | 1.42 |
| 3 | 1.66 | 12 | 3.38 | 0.08 | 1.41 |
| 4 | 1.66 | 18 | 3.38 | 0.08 | 1.45 |
| 5 | 1.39 | 3 | 3.92 | 0.15 | 2.06 |
| 6 | 1.39 | 7 | 3.92 | 0.12 | 1.59 |
| 7 | 1.39 | 12 | 3.92 | 0.11 | 1.57 |
| 8 | 1.39 | 18 | 3.92 | 0.12 | 1.60 |
| 9 | 0.825 | 3 | 5.05 | 0.33 | 2.72 |
| 10 | 0.825 | 7 | 5.05 | 0.27 | 2.28 |
| 11 | 0.825 | 12 | 5.05 | 0.27 | 2.23 |
| 12 | 0.825 | 18 | 5.05 | 0.27 | 2.24 |
| 13 | 0.413 | 3 | 5.87 | 0.63 | 3.86 |
| 14 | 0.413 | 7 | 5.87 | 0.56 | 3.45 |
| 15 | 0.413 | 12 | 5.87 | 0.55 | 3.38 |
| 16 | 0.413 | 18 | 5.87 | 0.55 | 3.40 |
| 17 | 0 | 3 | 6.70 | 1.17 | 5.49 |
| 18 | 0 | 7 | 6.70 | 1.17 | 5.49 |
| 19 | 0 | 12 | 6.70 | 1.17 | 5.49 |
| 20 | 0 | 18 | 6.70 | 1.17 | 5.49 |

**Table 5:** Results for transluminal pressure Case 3.

| Case | Plaque Thickness (mm) | Plaque Length (mm) | Inner Diameter (mm) | Area Compliance (ΔA/ΔP) ($mm^2$/torr) % | Diameter Compliance (DD/D/DP) $X10^4$ |
|---|---|---|---|---|---|
| 1 | 1.66 | 3 | 3.38 | 0.10 | 1.50 |
| 2 | 1.66 | 7 | 3.38 | 0.08 | 1.14 |
| 3 | 1.66 | 12 | 3.38 | 0.08 | 1.14 |
| 4 | 1.66 | 18 | 3.38 | 0..08 | 1.17 |
| 5 | 1.39 | 3 | 3.92 | 0.15 | 1.66 |
| 6 | 1.39 | 7 | 3.92 | 0.12 | 1.28 |
| 7 | 1.39 | 12 | 3.92 | 1.17 | 1.27 |
| 8 | 1.39 | 18 | 3.92 | 1.19 | 1.29 |
| 9 | 0.825 | 3 | 5.05 | 0.33 | 2.19 |
| 10 | 0.825 | 7 | 5.05 | 0.28 | 1.83 |
| 11 | 0.825 | 12 | 5.05 | 0.27 | 1.80 |
| 12 | 0.825 | 18 | 5.05 | 0.27 | 1.81 |
| 13 | 0.413 | 3 | 5.87 | 0.64 | 3.12 |
| 14 | 0.413 | 7 | 5.87 | 0.57 | 2.79 |
| 15 | 0.413 | 12 | 5.87 | 0.56 | 2.74 |
| 16 | 0.413 | 18 | 5.87 | 0.56 | 2.75 |
| 17 | 0 | 3 | 6.70 | 1.18 | 4.44 |
| 18 | 0 | 7 | 6.70 | 1.18 | 4.44 |
| 19 | 0 | 12 | 6.70 | 1.18 | 4.44 |
| 20 | 0 | 18 | 6.70 | 1.18 | 4.44 |

Future stages of the work will involve the reproduction of these results with patient-specific plaque measurements and extension from the general to the specific case will be made.

Regardless of the limitations, the results from the simplified plaque model are useful to quantify the degree of compliance change which is achieved for plaque removal. In fact, if compliance targets are available, they can be directly related to plaque removal so that procedures can be tailored to specific patient compliance objectives.

## Concluding Remarks

A numerical study was completed to quantify the effect of calcified plaque removal on artery compliance. The modeled artery segment was the proximal superficial femoral artery. Flow, pressure and geometry information was obtained from a patient before and after an orbital atherectomy procedure. The calculations were extended to

**Table 6:** Results for transluminal pressure Case 4.

| Case | Plaque Thickness (mm) | Plaque Length (mm) | Inner Diameter (mm) | Area Compliance (ΔA/ΔP) ($mm^2$/torr) % | Diameter Compliance (DD/D/DP) $X10^4$ |
|---|---|---|---|---|---|
| 1 | 1.66 | 3 | 3.38 | 0.11 | 1.20 |
| 2 | 1.66 | 7 | 3.38 | 0.08 | 0.92 |
| 3 | 1.66 | 12 | 3.38 | 0.08 | 0.91 |
| 4 | 1.66 | 18 | 3.38 | 0.08 | 0.94 |
| 5 | 1.39 | 3 | 3.92 | 0.16 | 1.34 |
| 6 | 1.39 | 7 | 3.92 | 0.12 | 1.03 |
| 7 | 1.39 | 12 | 3.92 | 0.12 | 1.02 |
| 8 | 1.39 | 18 | 3.92 | 0.12 | 1.03 |
| 9 | 0.825 | 3 | 5.05 | 0.35 | 1.76 |
| 10 | 0.825 | 7 | 5.05 | 0.30 | 1.48 |
| 11 | 0.825 | 12 | 5.05 | 0.29 | 1.44 |
| 12 | 0.825 | 18 | 5.05 | 0.29 | 1.45 |
| 13 | 0.413 | 3 | 5.87 | 0.68 | 2.50 |
| 14 | 0.413 | 7 | 5.87 | 0.61 | 2.24 |
| 15 | 0.413 | 12 | 5.87 | 0.60 | 2.19 |
| 16 | 0.413 | 18 | 5.87 | 0.60 | 2.20 |
| 17 | 0 | 3 | 6.70 | 1.26 | 3.56 |
| 18 | 0 | 7 | 6.70 | 1.26 | 3.56 |
| 19 | 0 | 12 | 6.70 | 1.26 | 3.56 |
| 20 | 0 | 18 | 6.70 | 1.23 | 3.48 |

a variety of plaque lengths and for a wide range of eternal pressure conditions which represent the surrounding tissue. The simulations included a sheath of supporting tissue as well.

It was found that progressive removal of plaque led to a large change in the compliance. It was also found that the changes were largely independence of the lesion length, however very short lesions (3 mm) exhibited a slight difference compared to longer lesions (7 mm and longer). These calculations allow clinicians to target atherectomy procedures to meet a compliance goal. For instance, for individual patients with non-compliant arteries, it is possible to create a compliance goal and to then tailor the amount of calcified plaque which must be removed to achieve that goal.

The calculations were compared with literature measurements of compliance and were found to be in agreement. To the authors' best knowledge, this is the first numerical compliance study which includes surrounding tissue and progressive changes in plaque.

The results presented here are also useful in interpreting other prior results such as [69], which use novel sensing techniques to measure intima-media thickness, diameter, strain and distensibility in arteries with a focus on potential plaque rupture.

## Acknowledgements

The authors gratefully acknowledge the support of Cardiovascular Systems Inc.

## References

1. Ku DN (1997) Blood Flow in Arteries Annu Rev Fluid Mech 29: 399-434.
2. Stehbens WE, Davis PF, Martin BJ (1990) Blood Flow in Large Arteries: Applications to Atherogenesis and Clinical Medicine Monograph Atheroscler Basel, Karger 15: 1-15.
3. Sabbah HN, Khaja F, Brymer JF, Hawkings ET, Stein PD (1990) Blood flow in the Coronary Arteries of Man: Relation to Atherosclerosis. Monograph Atheroscler Basel Karger 15: 77-90.
4. Friedman MH, Bargeron CB, Mark FF (1990) Variability of geometry, Hemodynamics and Intimal Response of Human Arteries. Monograph Atheroscler Basel Karger 15: 109-116.
5. Caro CG, Fitz-Gerald JM, Schroter RC (1971) Atheroma and Arterial Wall Shear Observation, Correlation, and Proposal of a Shear Dependent Mass Transfer Mechanism for Atherogenesis. Proc Rey Soc Lon B 177: 109-159.
6. Kamiya A, Togawa T (1980) Adaptive Regulation of Wall Shear Stress to Flow Change in the Canine Carotid Artery. Am J Physiol 239: H14-H21.
7. Zarins CK, Giddens DP, Bharadvaj BK, Sottiurai VS, Mabon RF, et al. (1983) Carotid Bifurcation Atherosclerosis Quantitative Correlation of Plaque Localization with Flow Velocity Profiles and Wall Shear Stress. Circulation Research 53: 502-514.
8. Ku DN, Giddens DP, Zarins CK, Glagov S (1985) Pulsatile Flow and Atherosclerosis in the Human Carotid Artery Bifurcation Positive Correlation Between Plaque Location and Low Oscillating Shear Stress: Arteriosclerosis 5: 293-302.
9. Sprague EQ, Steinbach BL, Nerem RM, Schwartz CJ (1987) Influence of a Laminar Steady-State Fluid-Imposed WWall Shear Stress on the Binding, Internalization, and Degradation of Low-Densiyt Lipoproteins by Cultured Arterial Endothelium. Circulation 76: 648-656.
10. Nerem RM (1990) Vascular Endothelial Response to Shear Stress. Monograph Atheroscler Basel, Karger 15: 117-124.
11. Lorthios S, Lagree PY, C Marc-Vergnes JP, Cassot F (2000) Maximal Wall Shear Stress in Arterial Stenosis: Application to Internal Carotid Arteries. J Biomech Eng 122: 661-666.
12. Khaled ARA, Vafai K (2003) The Role of Porous Media in Modeling Flow and Heat Transfer in Biological Tissues. Int J Heat Mass Transfer 46: 4989-5003.
13. Khanafer K, Vafai K (2006) The Role of Porous Media in Biomedical Engineering as Related to Magnetic Resonance Imaging and Drug Delivery. Heat Mass Transfer 42: 939-953.

14. Khakpour M, Vafai K (2008) A Critical Assessment of Arterial Transport Models. Int J Heat Mass Transfer 51: 807-822.

15. Abraham JP, Sparrow EM, Lovik RD (2008) Unsteady, three dimensional fluid mechanic Analysis of Blood Flow in Plaque-Narrowed and Plaque-Free Arteries. Int J Heat Mass Transfer 51: 5633-5641.

16. Stark JR, Gorman JM, Sparrow EM, Abraham JP, Kohler RE (2013) Controlling the Rate of Penetration of a Therapuetic Drug into the Wall of an Artery by Means of a Pressurized Balloon. J Biomech Sci Eng 6: 527-532.

17. Abraham JP, Sparrow EM, Gorman JM, Stark JR, Kohler RE (2013a) A Mass Transfer Model of Temporal Drug Deposition in Artery Walls. Int J Heat Mass Transfer 59: 632-638.

18. Abraham JP, Stark JR, Gorman JM, Sparrow EM, Kohler RE (2013b) A Model of Drug Deposition Within Artery Walls. J Medical Devices 6: 020902.

19. Wang S, Vafai K (2014) Analysis of Low Density Lipoprotein (LDL) Transport With in a Curved Artery. Ann Biomed Eng (in press).

20. Ellahi R, Rahman S, Nadeem U, Vafai K (2015) The Blood Flow of Prandtl Fluid Through a Tapered Stenosed Arteries in Permeable Walls with Magnetic Field. Comm Theo Phys (in press).

21. O'Rourke MF, Staessen JA, Vlachopoulos D, Duprez D, Plante GE (2002) Clinical Applications of Arterial Stiffness; Definitions and Reference Values. Am J Hypertension 15: 426-444.

22. Pannier BM, Avolio AP, Hoeks A, Mancia G, Takazawa K (2002) Methods and Devices for Measuring Arterial Compliance in Humans. Am J Hypertension 15: 743-753.

23. Woodcock JP, Morris SJ, Wells PNT (1975) Significance of the Velocity Impulse Response and Cross-Correlation of the Femoral and Popliteal Blood-Velocity/Time Waveforms in Disease of the Superficial Femoral Artery. Med Biol Engin 13: 813-818.

24. Baird RN, Bird DR, Clifford PC, Lusby RJ, Skidmore R, et al. (1980) Upstream Stenosis: Its Diagnosis by Doppler Signals form the Femoral Artery. Arch Surgery 115: 1316-1322.

25. Nicholls SC, Kohler TR, Martin RL, Neff R, Phillips DJ, et al. (1986) Diastolic Flow as a Predictor of Arterial Stenosis. J Vasc Surgery 3: 498-501.

26. Burnham SJ, Jacques P, Burnham CB (1992) Noninvasive Detection of Iliac Artery Stenosis in the Presence of Superficial Femoral Artery Obstruction. J Vasc Surgery 16: 45-452.

27. Risoe C, Wille S (1978) Blood Velocity in Human Arteries Measured by a Bidirectional ultrasonic Doppler flowmeter. Acta Physiol Scand 103: 370-378.

28. Mohajer K, Zhang H, Gurell D, Ersoy H, Ho B, et al. (2006) Superficial Femoral Artery Occlusive Disease Severity Correlates with MR Cine Phase-Contrast Flow Measurements. J Mag Res Imaging 23: 355-360.

29. Holland CK, Brown JM, Scoutt LM, Taylor KW (1998) Lower Extremity Volumetric Arterial Blood Flow in Normal Subjects. Ultrasound Med Biol 24: 1079-1086.

30. Macpherson DS, Evans DH, Bell PRF (1984) Common Femoral Artery Doppler Wave-Forms: A Comparison of Three Methods of Objective Analysis with Direct Pressure Measurements. Br J Surgery 71: 46-49.

31. Caputo GR, Masui T, Gooding GAW, Chang JM, Higgins CB (1982) Popliteal and Tibioperoneal Arteries: Feasibility of Two Dimensional Time-of-Flight MR Angiography and Phase Velocity Mapping. Cardiovascular Radiology 182: 387-392.

32. Johnston KW, Maruzzo BC, Cobbold SC (1977) Errors and Artifacts of Doppler Flowmeters and Their Solution. Arch Surgery 112:1335-1342.

33. Johnston KW, Kassam M, Koers J, Cobbold RSC, MacHattie D (1984) Comparative Study of Four Methods for Quantifying Doppler Ultrasound Waveforms from the Femoral Artery. Ultrasound Med Biol 10: 1-12.

34. Baker JD, Herbert Machleder HI, Skidmore R (1984) Analysis of Femoral Artery Doppler Signals by Laplace Transform Damping Method. J Vascular Surgery 1: 520-524.

35. Woodcock JP, Gosling RG, Fitzgerald DE (1972) A New Non-Invasive Technique for Assessment of Superficial Femoral Artery Obstruction. Br J Surgery 59: 226-231.

36. Spronk S, den Hoed PT, de Jonge LCW, van Dijk LC, Pattynama PMT (2005) Value of the Duplex Waveform at the Common Femoral Artery for Diagnosing Obstructive Aortoiliac Disease. J Vascular Surgery 42: 236-242.

37. Skidmore R, Woodcock JP (1980) Physiological Interpretations of Doppler-Shift Waveforms – I Theoretical Considerations. Ultrasound Med Biol 6: 7-10.

38. Tang D, Yang C, Huang Y, Ku DN (1999a) Wall Stress and Strain Analysis Using a Three-Dimensional Thick-Wall Model with Fluid-Structure Interactions for Blood Flow in Carotid Arteries with Stenosis. Computers and Structures 72: 341-356.

39. Tang D, Yang C, Ku DN (1999) A 3-D Thin-Wall Model with Fluid-Structure Interactions for Blood Flow in Carotid Arteries with Symmetric and Asymmetric Stenosis. Computers and Structures 72: 357-377.

40. Zhao SZ, Xu XY, Hughes AD, Thom SA, Stanton AV, et al. (2000) Blood Flow and Vessel Mechanics in a Physiologically Realistic Model of a Human Carotid Arterial Bifurcation. Journal of Biomechanics 33: 975-984.

41. Tang D, Yang C, Walker H, Kobayashi S, Ku DN (2002) Simulating Cyclic Artery Compression Using a 3D Unsteady Model with Fluid-Structure Interactions. Computers and Structures 80: 1651-1665.

42. Tang D, Yang C, Kobayashi S, Zheng J, Vito RP (2003) Effect of Stenosis Asymmetry on Blood Flow and Artery Compression: A Three-Dimensional Fluid-Structure Interaction Model. Ann Biomed Engin 31: 1182-1193.

43. Tang D, Yang C, Kobayashi S, Ku DN (2004) Effect of a Lipid Pool on Stress/Strain Distributions in Stenotic Arteries: 3-D Fluid-Structure Interactions (FSI) Models. J Biomech Engin 126: 363-370.

44. Li Z, Kleinstreuer C (2005) Blood Flow and Structure Interactions in a Stented Abdominal Aortic Aneurysm Model. Med Engin Physics 27: 369-382.

45. Torii R, Oshima M, Kobayashi T, Takagi K, Tezduyar TE (2006) Fluid-Structure Interaction Modeling of Aneurysmal Conditions with High and Normal Blood Pressures. Computational Mechanics 38: 482-490.

46. Valencia A, Villanueva M (2006) Unsteady Flow and Mass Transfer in Models of Stenotic Arteries Considering Fluid-Structure Interaction. Int Comm Heat Mass Transfer 33: 966-975.

47. Valencia A, Solis F (2006) Blood Flood Dynamics and Arterial Wall Interaction in a Saccular Aneurysm Model of the Basilar Artery. Computers and Structures 84: 1326-1337.

48. Torii R, Oshima M, Kobayashi T, Takagi K, Tezduyar TE (2007) Influence of Wall Elasticity in Patient Specific Hemodynamic Simulations. Computers and Fluids 36: 160-168.

49. Bluestein D, Alemu Y, Avrahami I, Gharib M, Dumont K, et al. (2008) Influence of Microcalcifications on Vulnerable Plaque Mechanics. J Biomech 41: 1111-1118.

50. Torii R, Oshima M, Kobayashi T, Takagai K, Tezduyar TE (2009) Fluid-Structure Interaction Modeling of Blood Flow and Cerebral Aneurysm: Significance of Artery and Aneurysm Shapes. Comp Meth Appl Mech Eng 198: 3613-3621.

51. Khanafer K, Bull JL, Berguer R (2009) Fluid-Structure Interaction of Turbulent Pulsatile Flow Within a Flexible Wall Axisymmetric Aortic Aneurysm Model. Euro J Mech B/Fluids 28: 88-102.

52. Janela J, Moura A, Sequeira A (2010) A 3D Non-Newtonian Fluid-Structure Interaction Model for Blood Flow in Arteries. J Comput Appl Mech 234: 2783-2791.

53. Kung EO, Les AS, Figueroa CA, Medina F, Arcaute K, et al. (2011) In Vitro Validation of Finite Element Analysis of Blood Flow in Deformable Models. Ann Biomed Eng 39: 1947-1960.

54. Croseetto P, Reymond P, Deparis S, Kontaxakis D, Stergiopulos N, et al.

(2011) Fluid-Structure Interaction Simulation of Aortic Blood Flow. Computers and Fluids 43: 46-57.

55. Malve M, Garcia A, Ohayon J, Martinez MA (2012) Unsteady Blood Flow and Mass Transfer of a Human Left Coronary Artery Bifurcation: FSI vs CFD. Int Comm Heat Mass Transfer 39: 745-751.

56. Reymond P, Crosetto P, Deparis S, Quarteroni A, Stergiopulos N (2013) Physiological Simulation of Blood Flow in the Aorta: Comparison of Hemodynamic Indices as Predicted by 3-D FSI, 3-D Rigid Wall and 1-D Models. Med Eng Physics 35: 784-791.

57. Liu Y, Dang C, Garcia M, Gregersen H, Kassab GS (2007) Surrounding Tissues Affect the Passive Mechanics of the Vessel Wall: Theory and Experiment. Am J Heart Circ Physiol 293: H3290-H3300.

58. Moireau P, Xiao N, Astorino M, Figueroa CA, Chapelle D, et al. (2012) External Tissue Support and Fluid-Structure Simulation in Blood Flows. Biomech Modeling i Mechanobiol 11: 1-18.

59. Sun B, Vallez LJ, Plourde BD, Stark JR, Abraham JP (2015) Influence of Supporting Tissue on the Deformation and Compliance of Healthy and Diseased Arteries. J Biomed Sc Eng 8: 590-599.

60. Zotz RJ, Erbel R, Philipp A, Judt A, Wagner H, et al. (1992) High-speed rotational angioplasty-induced echo contrast in vivo and in vitro optical analysis. Catheter Cardio Diag 26: 98-109.

61. Kini A, Marmur J, Duvvuri S, Dangas G, Choudhary S, et al. (1999) Rotational atherectomy: improved procedural outcome with evolution of technique and equipment Single-center results of first 1,000 patients. Catheter Cardio Interven 46: 305-311.

62. Tamashiro A, Villegas M, Tamashiro G, Enterrios D, Dini A, et al. (2008) Retrograde Rotablator in Limb Salvage: A New Technique Using an Open Approach. Cariodvascular Inter Radiol 29: 854-856.

63. Helgeson ZI, Jenkins J, Abraham JP, Sparrow EM (2011) Particle Trajectories and Agglomeration/Accumulation in Branching Arteries Subjected to Orbital Atherectomy. Open Biomed Eng J 5: 1108-1116.

64. Adams G, Khanna P, Staniloae C, Abraham JP, Sparrow EM (2011) Optimal Techniques with the Diamondback 360 System Achieve Effective Results for the Treatment of Peripheral Arterial Disease. J Cardiovascular Trans Res 4: 220-229.

65. Ramazani-Rend R, Chelikani S, Sparrow EM, Abraham JP (2010) Experimental and Numerical Investigation of Orbital Atherectomy: Absence of Cavitation. J Biomed Science Eng 3: 1108-1116.

66. Stanlioe CS, Korabathina R (2014) Orbital Atherectomy: Device Evolution and Clinical Data. J Invasive Cadiol 26: 215-219.

67. McVeigh GE, Bank AJ, Cohn JN (2007) Arterial Compliance, in Cardiovascular Medicine, edited by Willerson, JT, Wellens. HJJ, Cohn, JN, Holmes, DR, Springer 1811-1831.

68. Tai NRM, Giudiceandrea A, Salacinski HJ, Seifalian AM, Hamilton G (1999) In vivo femoropopliteal arterial wall compliance in subjects with and without lower limb disease. J Vasc Surgery 30: 936-945.

69. Paini A, Boutouyrie P, Calvet D, Zidi M, (2007) Multiaxial Mechanical Charactertistics of Carotid Plaque. Stroke 38: 117-123.



***Citation:*** *Vallez LJ, Sun B, Plourde BD, Abraham JP, Staniloae CS (2015) Numerical Analysis of Arterial Plaque Thickness and its Impact on Artery Wall Compliance. J Cardiovasc Med Cardiol 2(2): 026-034. DOI: 10.17352/2455-2976.000019*